Simulation of ideal inertial sensor measurements

Open Aided Navigation Project

Revision number 0.1

Dr. Fedor Baklanov
2020-12-04

Contents

1 Introduction

This document explains the software for IMU data simulation provided in the open source project Open Aided Navigation.

Some explanations, such as coordinate frame definitions, notation, etc. are omitted in this document. A reader is encouraged to have a look into the *Documentation_InsGnssFilterLoose.pdf* that is available for download in the Bitbucket repository.

2 Principles of inertial navigation

Accelerometers and gyroscopes are usually called inertial sensors. An accelerometer is a sensor that measures one or more projections of a specific force acting on a body. A gyroscope is a device for measuring projections of an angular rate of the body relatively to some inertial coordinate frame. Nowadays the abovementioned sensors are usually rigidly attached to the moving object which is why the measured values present the projections onto a body-fixed coordinate frame (Farrell, 2008).

The core idea of inertial navigation consists in determining position and orientation of a moving object by means of integrating numerically differential equations of motion of a point mass in the neighborhood of Earth. Angular rate and specific force present inputs to the dynamic system and need to be measured by onboard inertial sensors. Additionally, initial position, velocity, and orientation are required to be known (Farrell, 2008).

The paragraphs above were taken from https://navigation-expert.com/inertial_navigation.

3 What is ideal IMU data?

Inertial navigation is a powerful tool for position, velocity, and orientation estimation. Its advantages are:

- Availability of output at high rates
- No dependency to external signals, such as signals of GNSS
- Smoothness of output signals
- High level of robustness

However, in practice inertial navigation has some limitations. Due to presence of instrumental errors, such as offsets and noise, coordinates, provided by an inertial navigation system (INS) start to diverge from the true user location. For most modern MEMS inertial sensors divergence rate appears high and resembles “unbounded drift”. Nevertheless, IMU instrumental errors are not the only factor that contributes to error growth. Another important factor is accuracy of *the numerical method* employed to integrate INS ordinary differential equation. Even with the best available sensors, such as ring-laser gyroscopes, INS would “drift” relatively fast if the simplest 1st order Euler method was used for integration.

That being said, how could we define “ideal” IMU measurements? *From the perspective of inertial navigation, IMU measurements would be ideal if they allowed to reconstruct vehicle’s trajectory and orientation perfectly.* At this place it is important to add that this should be fulfilled only when sufficiently accurate numerical method is used and when integration step is small enough.

4 Simulation of ideal inertial measurements

Motion of a point mass in the neighborhood of Earth can be modeled by the ordinary differential equation given below. This equation and its derivation can be found in the book (Farrell, 2008).

$$
\begin{aligned}
\dot{\mathbf{x}}_e &= \mathbf{v}_e \\
\dot{\mathbf{v}}_e &= -2[\boldsymbol{\omega}_{ie}\times]\mathbf{v}_e + \mathbf{g}_e(\mathbf{x}_e) + \mathbf{C}_{es}(\breve{\mathbf{q}}_{es})\mathbf{f}_s \\
\dot{\breve{\mathbf{q}}}_{es} &= \frac{1}{2}(\breve{\mathbf{q}}_{es} * \breve{\boldsymbol{\omega}}_{is} - \breve{\boldsymbol{\omega}}_{ie} * \breve{\mathbf{q}}_{es})
\end{aligned}
\tag{4.1}
$$

Herein

- $\mathbf{x}_e$ is a 3×1 vector of coordinates of a vehicle in the ECEF coordinate system
- $\mathbf{v}_e$ is a 3×1 column whose elements are projections of the velocity relative to ECEF frame onto basis vectors of the ECEF frame
- $\breve{\mathbf{q}}_{es}$ is a rotation quaternion that defines coordinate transformation from the sensor frame (s-frame) to the ECEF frame (e-frame)
- $\mathbf{f}_s$ is specific force
- $\breve{\boldsymbol{\omega}}_{is}$ is a quaternion, whose scalar part is zero, and vector part is angular rate of the sensor frame relative to the quasi-inertial coordinate frame
- $\breve{\boldsymbol{\omega}}_{ie}$ is a quaternion, whose scalar part is zero, and vector part is angular rate of the e-frame relative to the i-frame
- $\mathbf{g}_e(\mathbf{x}_e)$ is gravity vector

The equation (4.1) can be used to express specific force and angular rate in terms of position, orientation, and their derivatives. Rearranging (4.1) yields

$$
\begin{aligned}
\mathbf{f}_s &= \mathbf{C}_{es}^{-1}\left(\dot{\mathbf{v}}_e + 2[\boldsymbol{\omega}_{ie}\times]\mathbf{v}_e - \mathbf{g}_e(\mathbf{x}_e)\right) \\
\breve{\boldsymbol{\omega}}_{is} &= \breve{\mathbf{q}}_{es}^{-1} * \left(2 \cdot \dot{\breve{\mathbf{q}}}_{es} + \breve{\boldsymbol{\omega}}_{ie} * \breve{\mathbf{q}}_{es}\right)
\end{aligned}
\tag{4.2}
$$

Consider now timeseries $\mathbf{x}_e(t_k)$ and $\breve{\mathbf{q}}_{es}(t_k)$ are provided by some vehicle simulator (for example, X-Plane flight simulator) or measured by a navigation system in a test.
Then the following procedure can be employed to simulate ideal IMU measurements and a reference trajectory that corresponds to the measurements.

1. Downsample the timeseries $\mathbf{x}_e(t_k)$ and $\breve{\mathbf{q}}_{es}(t_k)$.
    a. *This will help to "smoothen" the reference trajectory and generated inertial measurements will not have small high-frequency oscillations.*
2. Derive Euler angles timeseries $\varphi(t_k)$, $\vartheta(t_k)$, and $\psi(t_k)$ from the quaternion timeseries $\breve{\mathbf{q}}_{es}(t_k)$, unwrap range rollovers, if necessary.
3. Do spline interpolation of the position and Euler angles timeseries. Choose <u>*at least*</u> the third order spline.
    a. *Euler angles should be preferred for interpolation, because splines cannot ensure that interpolated quaternion will remain an <u>orientation quaternion</u>, i. e. that its norm will remain 1 after interpolation.*
    b. *After interpolation position and orientation splines will be available. Note that splines of the order 3 and higher have 2 continuous derivatives. <u>So, velocity can be derived from the position spline exactly</u>. No inaccurate numerical differentiation needs to be employed. The derived velocity vector will be continuous. The same applies to the derivatives of Euler angles.*
4. Choose desired time grid τ_i, $i = \overline{1, N}$. <u>*Any IMU data frequency is possible*</u>.
5. Differentiate position spline $\mathbf{x}_e^{sp}$ two times to obtain velocity spline $\mathbf{v}_e^{sp}$ and acceleration spline $\dot{\mathbf{v}}_e^{sp}$.
6. Differentiate Euler angles splines φ^{sp}, ϑ^{sp}, and ψ^{sp} to get the splines $\dot{\varphi}^{sp}$, $\dot{\vartheta}^{sp}$, and $\dot{\psi}^{sp}$.
7. Evaluate the splines $\mathbf{x}_e^{sp}$, $\mathbf{v}_e^{sp}$, φ^{sp}, ϑ^{sp}, and ψ^{sp} at times τ_i, $i = \overline{1, N}$. <u>*This will yield reference position, velocity, and orientation*</u>.
8. Evaluate the splines $\dot{\mathbf{v}}_e^{sp}$, $\dot{\varphi}^{sp}$, $\dot{\vartheta}^{sp}$, and $\dot{\psi}^{sp}$ at times τ_i, $i = \overline{1, N}$. This will yield auxiliary values $\dot{\mathbf{v}}_e(\tau_i)$, $\dot{\varphi}(\tau_i)$, $\dot{\vartheta}(\tau_i)$, and $\dot{\psi}(\tau_i)$.
9. Derive $\dot{\breve{\mathbf{q}}}_{es}(\tau_i)$ form the reference Euler angles and their derivatives obtained in the steps 7 and 8. See formula (4.4) for details.

10. Use the equation (4.2) to compute $\mathbf{f}_s(\tau_i)$ and $\breve{\boldsymbol{\omega}}_{is}(\tau_i)$. Needed inputs: reference position, velocity, and orientation from the step 7, $\dot{\mathbf{v}}_e(\tau_i)$ from the step 8, $\dot{\breve{\mathbf{q}}}_{es}(\tau_i)$ from the step 9.
    a. Note that the scalar part of the quaternion $\breve{\boldsymbol{\omega}}_{is}(\tau_i)$ will be zero, while the vector part is the desired angular rate $\boldsymbol{\omega}_{is}(\tau_i)$

Conversion of Euler angles to a quaternion is given by

$$\begin{aligned}
q_{es0} &= \cos\frac{\varphi}{2}\cos\frac{\vartheta}{2}\cos\frac{\psi}{2} + \sin\frac{\varphi}{2}\sin\frac{\vartheta}{2}\sin\frac{\psi}{2} \\
q_{es1} &= \sin\frac{\varphi}{2}\cos\frac{\vartheta}{2}\cos\frac{\psi}{2} - \cos\frac{\varphi}{2}\sin\frac{\vartheta}{2}\sin\frac{\psi}{2} \\
q_{es2} &= \cos\frac{\varphi}{2}\sin\frac{\vartheta}{2}\cos\frac{\psi}{2} + \sin\frac{\varphi}{2}\cos\frac{\vartheta}{2}\sin\frac{\psi}{2} \\
q_{es3} &= \cos\frac{\varphi}{2}\cos\frac{\vartheta}{2}\sin\frac{\psi}{2} - \sin\frac{\varphi}{2}\sin\frac{\vartheta}{2}\cos\frac{\psi}{2}
\end{aligned} \tag{4.3}$$

Thus,

$$\begin{aligned}
\dot{q}_{es0} = 0.5 \cdot \Big(&-\sin\frac{\varphi}{2}\cos\frac{\vartheta}{2}\cos\frac{\psi}{2}\cdot\dot{\varphi} - \cos\frac{\varphi}{2}\sin\frac{\vartheta}{2}\cos\frac{\psi}{2}\cdot\dot{\vartheta} + \cos\frac{\varphi}{2}\cos\frac{\vartheta}{2}\sin\frac{\psi}{2}\cdot\dot{\psi} \\
&+ \cos\frac{\varphi}{2}\sin\frac{\vartheta}{2}\sin\frac{\psi}{2}\cdot\dot{\varphi} + \sin\frac{\varphi}{2}\cos\frac{\vartheta}{2}\sin\frac{\psi}{2}\cdot\dot{\vartheta} + \sin\frac{\varphi}{2}\sin\frac{\vartheta}{2}\cos\frac{\psi}{2}\cdot\dot{\psi}\Big) \\
\dot{q}_{es1} = 0.5 \cdot \Big(&\cos\frac{\varphi}{2}\cos\frac{\vartheta}{2}\cos\frac{\psi}{2}\cdot\dot{\varphi} - \sin\frac{\varphi}{2}\sin\frac{\vartheta}{2}\cos\frac{\psi}{2}\cdot\dot{\vartheta} - \sin\frac{\varphi}{2}\cos\frac{\vartheta}{2}\sin\frac{\psi}{2}\cdot\dot{\psi} \\
&+ \sin\frac{\varphi}{2}\sin\frac{\vartheta}{2}\sin\frac{\psi}{2}\cdot\dot{\varphi} - \cos\frac{\varphi}{2}\cos\frac{\vartheta}{2}\sin\frac{\psi}{2}\cdot\dot{\vartheta} - \cos\frac{\varphi}{2}\sin\frac{\vartheta}{2}\cos\frac{\psi}{2}\cdot\dot{\psi}\Big) \\
\dot{q}_{es2} = 0.5 \cdot \Big(&-\sin\frac{\varphi}{2}\sin\frac{\vartheta}{2}\cos\frac{\psi}{2}\cdot\dot{\varphi} + \cos\frac{\varphi}{2}\cos\frac{\vartheta}{2}\cos\frac{\psi}{2}\cdot\dot{\vartheta} - \cos\frac{\varphi}{2}\sin\frac{\vartheta}{2}\sin\frac{\psi}{2}\cdot\dot{\psi} \\
&+ \cos\frac{\varphi}{2}\cos\frac{\vartheta}{2}\sin\frac{\psi}{2}\cdot\dot{\varphi} - \sin\frac{\varphi}{2}\sin\frac{\vartheta}{2}\sin\frac{\psi}{2}\cdot\dot{\vartheta} + \sin\frac{\varphi}{2}\cos\frac{\vartheta}{2}\cos\frac{\psi}{2}\cdot\dot{\psi}\Big) \\
\dot{q}_{es3} = 0.5 \cdot \Big(&-\sin\frac{\varphi}{2}\cos\frac{\vartheta}{2}\sin\frac{\psi}{2}\cdot\dot{\varphi} - \cos\frac{\varphi}{2}\sin\frac{\vartheta}{2}\sin\frac{\psi}{2}\cdot\dot{\vartheta} + \cos\frac{\varphi}{2}\cos\frac{\vartheta}{2}\cos\frac{\psi}{2}\cdot\dot{\psi} \\
&- \cos\frac{\varphi}{2}\sin\frac{\vartheta}{2}\cos\frac{\psi}{2}\cdot\dot{\varphi} - \sin\frac{\varphi}{2}\cos\frac{\vartheta}{2}\cos\frac{\psi}{2}\cdot\dot{\vartheta} + \sin\frac{\varphi}{2}\sin\frac{\vartheta}{2}\sin\frac{\psi}{2}\cdot\dot{\psi}\Big)
\end{aligned} \tag{4.4}$$

5 Example

The script *sim_imuAndRef.m* from the Open Aided Navigation repository implements the simulation procedure presented in the Section 4. By default, the script simulates ideal IMU measurements at 100Hz. Figures 1–3 show deviations from reference of position, velocity, and orientation computed from the simulated IMU measurements by means of numerical integration of the differential equation (4.1) using Heun's 2nd order method. Orientation errors are of magnitude 10^{-5} [rad], velocity errors are on centimeter per second level, position errors get close to 15 meters.

Next, Figures 4–9 *show INS errors for IMU data simulated at 25 and 50Hz rate. Note that each time when sensor rate gets 2 times lower, INS errors become exactly factor 4 larger. This effect is due to accuracy of the Heun's method, which is a second order method. It means that decreasing/increasing integration step linearly should result into accuracy improving/degrading quadratically.*

The observed effect serves as an evidence of IMU data being "ideal", because residual INS errors can be explained by numerical effects. Choice of smaller step size and employment of more accurate integration method will mitigate inevitable error accumulation considerably.

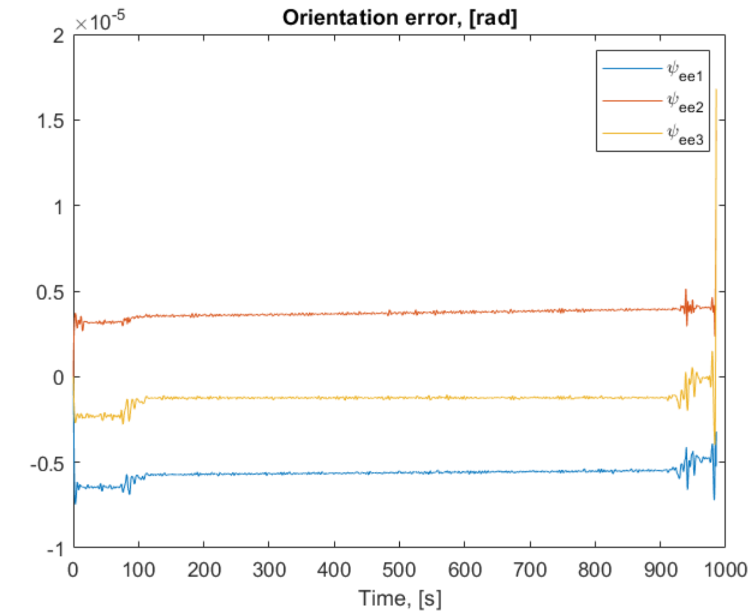

Figure 1: 100Hz

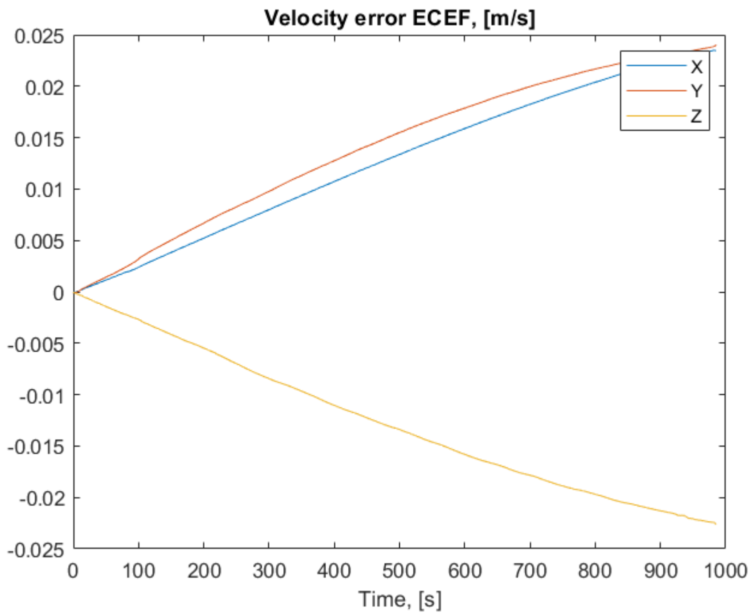

Figure 2: 100Hz

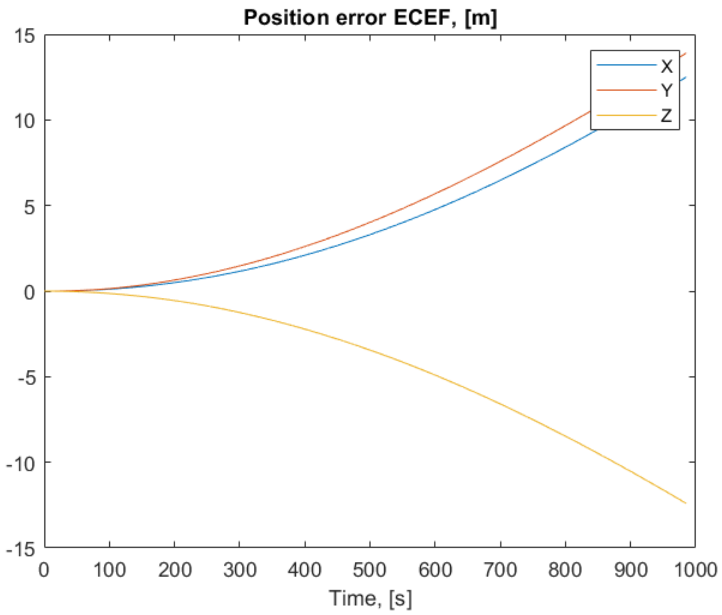

Figure 3: 100Hz

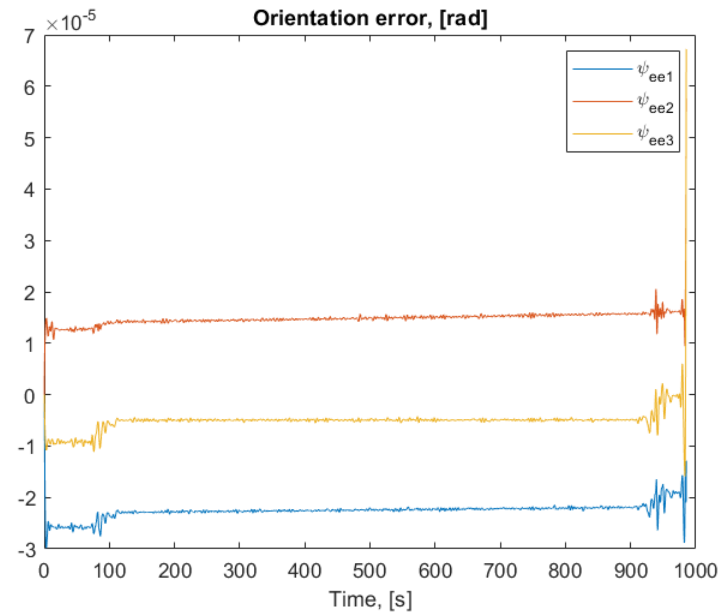

Figure 4: 50Hz

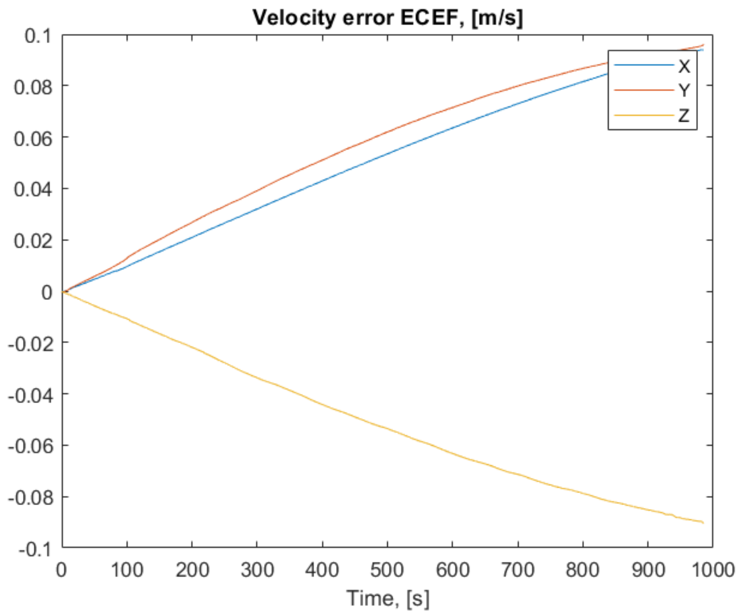

Figure 5: 50Hz

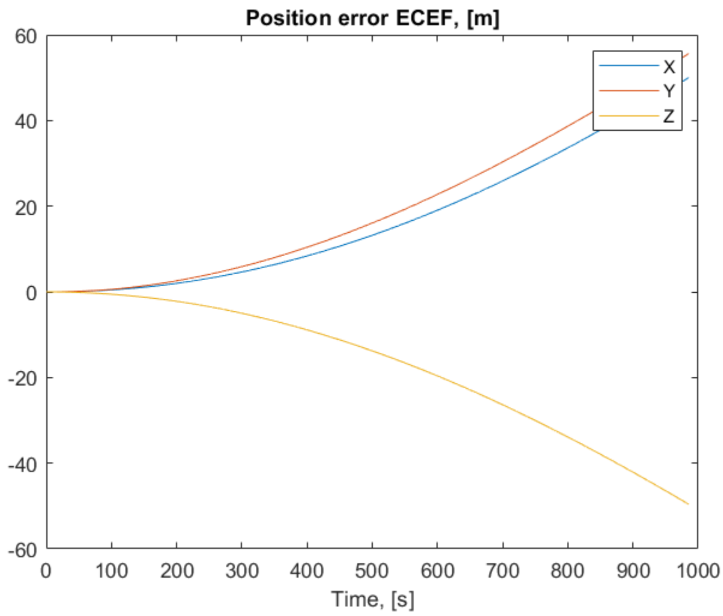

Figure 6: 50Hz

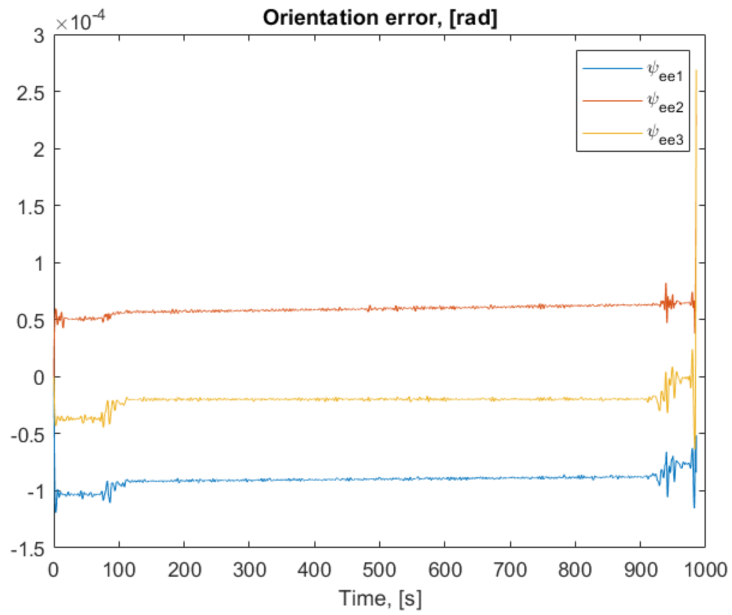

Figure 7: 25Hz

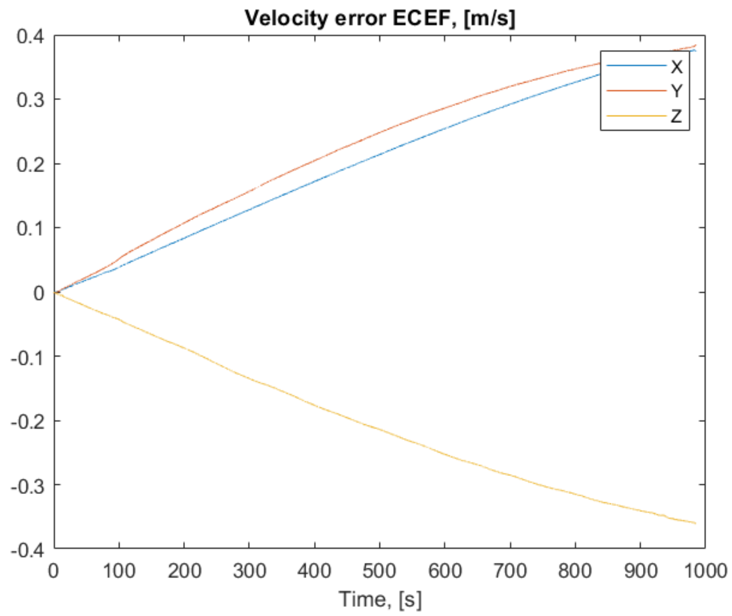

Figure 8: 25Hz

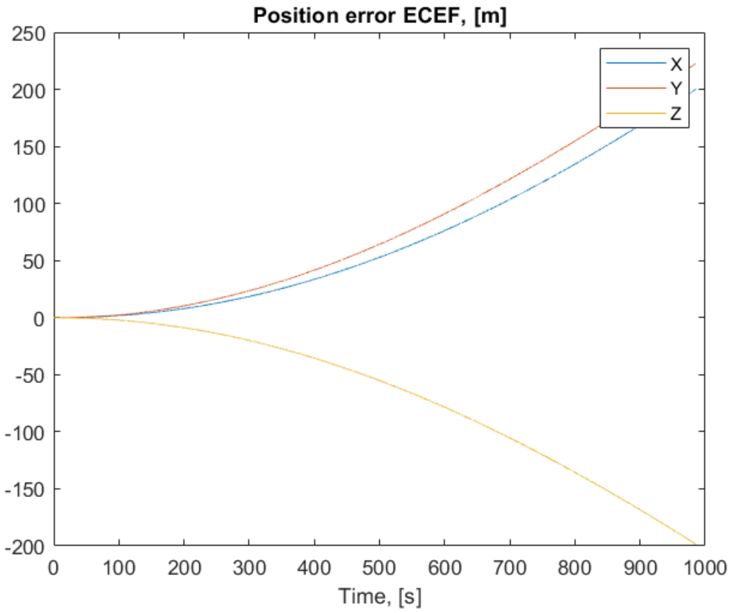

Figure 9: 25Hz

6 Bibliography

Baklanov, F. (2020, 12 2). *Inertial navigation*. Retrieved from navigation-expert.com: https://navigation-expert.com/inertial_navigation

Farrell, J. (2008). *Aided Navigation: GPS with High Rate Sensors.* McGraw-Hill.